Current Chemistry Letters 12 (2023) 477–488

Contents lists available atGrowingScience

Current Chemistry Letters

homepage: www.GrowingScience.com

3-Difluormethyl-5-carbomethoxy-2,4-pyrazole: Molecular mechanism of the formation and molecular docking study

Ali Barhoumi[a], Najia Ourhriss[b], Mohammed Elalaoui Belghiti[c,d], Mohammed Chafi[e], Asad Syed[f], Rajalaksh-manan Eswaramoorthy[g], Meenakshi Verma[h], Abdellah Zeroual[a*], Karolina Zawadzińska[i], Radomir Jasiński[i]

[a]*Molecular Modelling and Spectroscopy Research Team, Faculty of Science, Chouaïb Doukkali University, P.O. Box 20, 24000 El Jadida, Morocco*
[b]*Laboratory of Biomolecular Chemistry, Natural Substances and Reactivity, URAC 16, Faculty of Sciences Semlalia, Cadi Ayyad University, P.O. Box 2390, Marrakech, Morocco*
[c]*Laboratory of Physical Chemistry of Materials, Ben M'Sick Faculty of Sciences, Hassan II University, Casa-blanca, Morocco*
[d]*Laboratory of Nernest Technology, 163 Willington Street, Sherbrooke, QC J1H5C7, Canada*
[e]*LIPE, Higher School of Technology, Hassan II University of Casablanca, B.P 8012 Oasis, Morocco*
[f]*Department of Botany and Microbiology, College of Science, King Saud University, P.O. Box 2455 Riyadh 11451, Saudi Arabia*
[g]*Department of Prosthodontics, Saveetha Dental College and Hospitals, Saveetha Institute of Medical and Technical Sciences (SIMATS), Chennai-600 077, India*
[h]*University Centre for Research & Development, Department of Chemistry, Chandigarh University, Gharuan, Mohali, India*
[i]*Department of Organic Chemistry and Technology, Cracow University of Technology, Warszawska 24, 31-155 Cracow, Poland*

C H R O N I C L E

Article history:
Received December 20, 2022
Received in revised form
January 28, 2023
Accepted March 28, 2023
Available online
March 28, 2023

Keywords:
[3+2] cycloaddition
Difluoromethyldiazomethane
Methyl propynoate
Molecular Electron Density Theory
MEDT
Covid-19

A B S T R A C T

Application of the Molecular Electron Density Theory (MEDT) for the exploration of the [3+2] cycloaddition processes between methyl propynoate 1 and difluoromethyldiazomethane T-1, have been implemented using the DFT/B3LYP/6-311(d,p) level of theory. According to an examination of conceptual DFT indices, difluoromethyldiazomethane (T-1) participates in this reaction as a nucleophile, while methyl propynoate (1) should be considered as an electrophile. This cyclization is regiospecific, as evidenced by the activation and reaction energies, this agrees with the experiment's findings. It was discovered throughout ELF analysis that analyzed [3+2] cycloaddition is realised by a two-step mechanism. In addition, study of interactions of the products studied in this paper with the protein protease Covid-19 (PDB ID: 7R98) were carried out, by means of molecular docking study). The results indicate that the occurrence of the transfer of the proton to the nitrogen atom, increases the affinity of these products to the protein (**CA32-F1** and **CA32-F2**).

1. Introduction

Pyrazole is a five-atom heterocyclic organic molecule containing two nitrogen atoms and three carbon atoms disposed inside a ring structure. It is an organic building block, commonly used in the synthesis of various drugs, herbicides and dyes [1-3]. Pyrazole has a distinctive aroma and is used as a flavoring and fragrance ingredient in food industry and personal care products[4-6]. It has a characteristic reactivity, and its electron richness makes it useful in a variety of organic reactions[3]. Additionally, the pyrazole has been used as a reactant in contemporary synthetic reactions and as pharmaceutical and agricultural medicines[7, 8]. They are a part of the azole family of chemicals, one of the most well-studied classes. The numerous synthetic techniques and analogs of pyrazole, have been described in recent years[9-12]. The pyrazole ring exists in

* Corresponding author.
E-mail address zeroualabdellah2@gmail.com (A. Zeroual)

doi: 10.5267/j.ccl.2023.3.008

many compounds, which results in a wide range of uses in diverse industries, including technology and medicine[13-14]. They are specifically described as anti-bacterial[15], antifungal[16], anticancer[17], antidepressant[18], anti-inflammatory[19], antitubercular [20], antioxydants[21], and antiviral agents as well as inhibitors of protein glycation[22].

The most universal[23-31] strategy for the preparation of pyrazoles is undoubtedly, the [3+2] cycloaddition (32CA) processes with the participation of analogs of the diazomethane as three atom components (TAC) and 2 unsaturated components. In the light of the Molecular Electron Density Theory (MEDT)[32], 32CA have been categorized as the few types of reaction: pmr, pdr, cb, and zw[33], depending on the electronic structure of the fundamental TAC. The pdr type reactions are attained, the zw-type reactions require enough nucleophile/electrophophile activations to take place[34]. MEDT explicitly says that an electron density describes the molecular reactivity, in this context, several chemical reactions have been studied, to be specific [3+2][32-35] cycloadditions, [4+2] cycloaddition[36-37], the epoxidation reaction[38-41], thermal elimination reactions[42-43] and the reaction of nitration[44]. We have established that the MEDT theory provides more information than the FMO theory (Frontier Molecular Orbital Theory)[45].

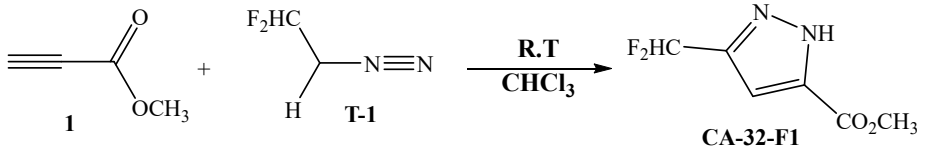

Scheme 1. The synthesic protocol for the preparation of 3-difluormethyl-5-carbomethoxy-2,4-pyrazole proposed by Mykhailuk.

Some time ago, Mykhailiuk[46] reported, that the reaction of difluoromethyl-diazomethane (**T-1**) and methyl propynoate (**1**) lead to pyrazole molecular system **CA-32-F1** (**Scheme 1**). So, it is evidential, that this is not the product of the direct cycloaddition reaction, but the result of the further transformation of primary formed adduct. Un-fortunately, these issues were not explained within the mentioned work. Many possible routes should be considered, including 32CA and further rearrangement, as well as the tautomerization of diazocompound in to nitrilimine, which can act as TAC with the alkyne 1. Moreover, the mechanism of the cycloaddition cannot be established a'priori. According to the actual state several mechanisms should be considered regarding to 32CA reactions: (a) non-polar mechanisms (synchronical mechanism or stepwise, bi-radical mechanism[47-48], (b) polar mechanisms (one step-two stage mechanism[49-50], (c) stepwise zwitterionic mechanism[51-53]. Additionaly, zwitterionic or biradical adducts with "extended conformation" may exist in a reaction environmently independent of [3+2] cycloadducts[54]. This study, which we performed is based on analysis of interactions between addents, as well as, results of the full exploration of possible reaction channels. In the addition to the following study, we also performed a molecular docking study for the possible products in this reaction (**Fig. 1**) to determine their potential biological activity.

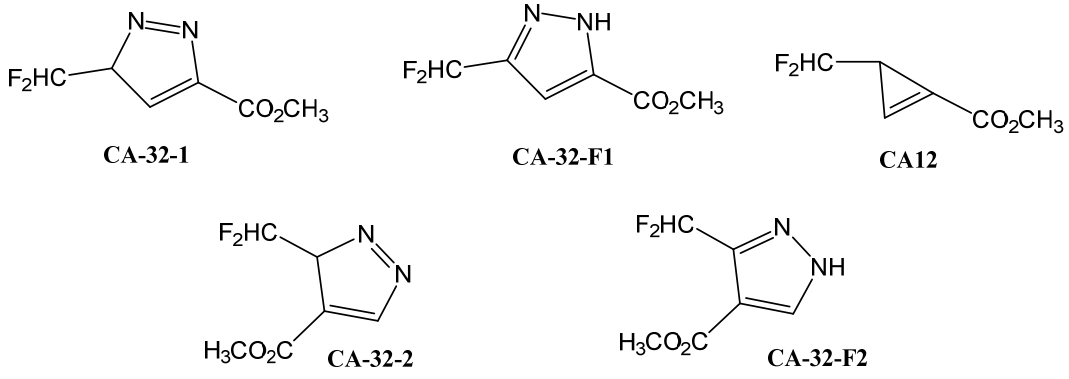

Fig. 1. 3-Difluormethyl-5-carbomethoxy-2,4-pyrazole and its derivatives in the following work.

2. Computational details

DFT (Density Functional Theory) is a theoretical method of quantum chemistry calculations that permits the description of molecular systems' electronic and en-ergetic properties. It is characterized as a compromise approach between *ab initio* quantum theory, which is very costly in terms of computation tempo, and classical chemistry methods, which are limited in their ability to describe electronic properties. B3LYP is a functional of the DFT theory that has been utilized to describe the molecular systems' electrical and energetic characteristics[51]. The basis 6-311(d,p) was ap-plied to characterize the electron distribution in molecules[56]. All the calculations are processed in Gaussian 09[57], which is quantum chemistry calculation software that was developed by Gaussian Inc. The IRC has been employed to follow the reaction path from its initial state

to its final state; it also enables the determination the intermediate steps of a chemical reaction and the associated activation barriers. To account for the effect of the solvent on the optimized structures, we employed Tomas' PCM (Polarizable Continuum Model)[58-63].

Global electronic properties of reactants were estimated according to the equations recommended by *Parr* and *Domingo* [64]. In particular, the electronic chemical potentials (μ) and chemical hardness (η) were evaluated in terms of one-electron energies of FMO (EHOMO and ELUMO) using the following equations:

$$\mu \approx (E_{HOMO}+E_{LUMO})/2 \quad (1)$$

$$\eta \approx E_{LUMO}-E_{HOMO} \quad (2)$$

Next, the values of μ and η were then used for the calculation of global electro-philicity (ω) according to the formula (3) and the global nucleophilicity (N)[65] can be expressed in terms of Eq. (4).

$$\omega=\mu^2/2\,\eta \quad (3)$$

$$N=E_{HOMO}-E_{HOMO\,(tetracyanoethene)} \quad (4)$$

Parr functions have been employed to find local indices, which are basic spin wave functions that are used in quantum chemistry to describe the electronic spin distribution in molecules[66, 67].

The electron localization function was described employing a Topmod software (ELF), this ELF is used to provide a representation of the distribution of electrons and electron cavities in the molecules[68-69].

3. Results and discussion

3.1. CDFT study

Analysis of the reactivity indices provided by CDFT is an efficient method for comprehending the reactivity of organic compounds, as demonstrated by several studies on chemical reactions. Electrophilicity, nucleophilicity, chemical hardness, and electronic chemical potential, which are the global indices listed in **Table 1** are exam-ined in order to prediction of the reactivity of difluoromethyldiazomethane (**T-1,T-2**) and methyl propynoate **1** in the cycloadition reaction.

Table. 1. Global electronic properties of methyl propynoate 1 and TACs (T-1 and T-2), as calculated in B3LYP/6-31G(d) (in eV).

Molecule	η	μ	ω	N
1	6.43	-4.42	1.51	1.89
T1	4.74	-4.19	1.85	2.96
T2	5.84	-3.96	1.34	2.64

The 32CA regioselectivity involves methyl propynoate (**1**) and difluoromethyldiazomethane (**T-1**) was investigated based on the reactants' CDFT reactivity indices. **Table 1** shows that the electronic chemical potential of T-1 ($\boldsymbol{\mu}$ = -4.19 eV) is lower, in absolute value, than that of methyl propynoate (1) ($\boldsymbol{\mu}$ = -4.42 eV), the global electron density transfer (GEDT) proceeds from **T-1** to **1**. On the other hand, the electronic chemical potential of **T-2** ($\boldsymbol{\mu}$ = -3,96 eV) has higher value than **1**, so the GEDT here should be considered in the same way as **T-1**.

Methyl propynoate's (**1**) electrophilicity and nucleophilicity indices are calculated as = 1.51 eV and N = 1.89 eV, respectively. As a result, **1** can be categorized both as a moderate nucleophile and as a strong electrophile. (**T-1** has an N nucleophilicity equal to 2.96 eV and $\boldsymbol{\omega}$ electrophilicity equal 1.85 eV, it could be classified as a strong nucleophile and as a moderate electrophile. Clearly, methyl propynoate (**1**) will engage in this reaction as an electrophile and difluoromethyldiazomethane (**T-1**) will engage in this reaction as a nucleophile. According to the actual classifications[70], the considered process should be treated as a polar process with Forward Electron Density Flux (FEDF). Almost the same we can establish for the compound **T-2**. The nucleophilicity index is 2.64 eV and electrophilicity index is 1.34 eV, which indicates that the chemical character of **T-2** is similar to **T-1**, but it is definitely weaker. The reaction between **1** and **T-2** should be also considered as FEDF. To examine the regioselectivity in polar reactions, Domingo et al. proposed the concept of electrophilic and nucleophilic Parr functions. These functions were designed to provide a measure of the electrophilic or nucleophilic character of a molecule or a chemical species, and they are used in computational chemistry to study chemical reactions and local properties of substances. The results revealed that the C1 atom's nucleophilic Parr function P_{C1}^{-}, is greater than N2 in difluoromethyldiazomethane (**T-1**); however, the C3 atom in methyl propynoate has an electrophilic Parr function (P_k^+) value of 0.45, which is obviously higher than the C2 atoms' equivalent value (0.00), this outcome is fairly consistent with the experiment, because it shows that the C3 atom of methyl propynoate 1 is the most electrophilic center.

This interaction will therefore occur amid the C3 carbon of methyl propynoate (**1**) and the C1 carbon of difluoromethyldiazomethane (**T-1**), resulting the formation of the product **P-1**.

3.2. ELF reagent characterization

Savin et al. are the ones who initially introduced the electron localization function (ELF) in the 1990s as a tool for visualizing and determining the localization of electrons in solids and molecules. The ELF provides a spatial representation of the electron density and enables researchers to study the distribution of electrons in chemical systems and to identify regions of electron localization and delocalization. Since its introduction, the ELF has been applied to a wide range of systems, including molecules, solids, surfaces, and materials, and has become a widely used tool in computational chemistry and materials science. The electron localization function (ELF), localize the electron pair in the spirit of Lewis structures. In particular, it helps in comprehending an empirical concept of electron localization. To identify the electrical structure of the reagents, (TACs **T-1** and **T-2**) and methyl propynoate **1**, we conducted an ELF topological study. This section describes the main ELF constituents and their relationship with chemical ideas. The ELF localization domains and valence basin populations are prearranged in (**Fig. 2**).

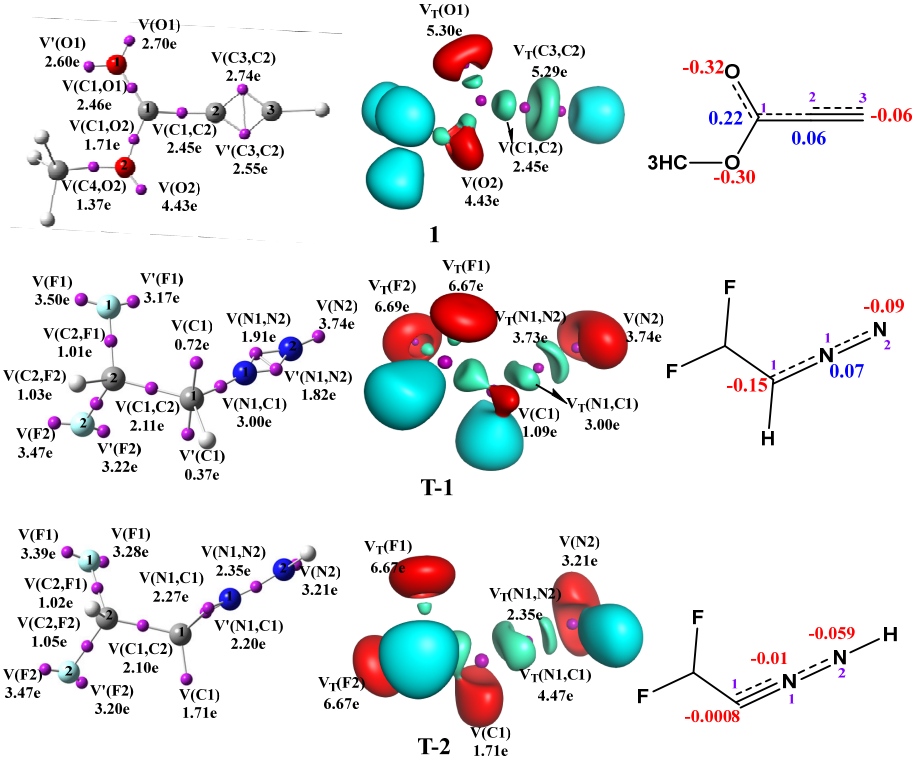

Fig. 2. ELF localization domains with the highest population of valence basins (red color: monosynaptic basin; green disynaptic basins; purple color: central atom and blue color: the surface of hydrogen atom)**.**

In the methyl propynoate molecule (**1**), there are four most important bisynaptic basins: two are located between carbons C2 and C3 with value V(C3,C2)=2.74e and V'(C3,C2)=2.55e, assimilating in total V_T(C2,C3)=5.29e, which shows the existence of a semi-triple bond between carbons C2 and C3. Two others, are located between carbon C1 and carbon C2 with value 2.45e, and between carbon C1 and oxygen O1 with value 2.46e, we also notice the existence of two monosynaptic basins gated by oxygen O1, integrating in total V_T(O1)=5. 30e. These values indicate that there is a delocalization of electrons on bonds O1-C1, C1-C2 and C2-C3, as it shows the Lewis structure of methyl propynoate **1**, this delocalization explains the great reactivity of the bond C2-C3.

In the structure of difluoromethyldiazomethane (tautomer **T-1**), there are three relevant bisynaptic basins: two are located between the two nitrogen atoms of total value V_T(N1,N2)=3.73e and the third bisynaptic basin is placed at a distance between the nitrogen atom N1 and the carbon atom C1 of value V(N1,C1)=3.00e, which there are semi double bonds between the three centers of the TAC as mentioned in the Lewis structure. The two fluorescent atoms have two monosynaptic basins integrating in total to 6.67e, so there are more than six electrons around each fluorescent atom, which makes the TAC very reactive, this high reactivity of TAC was also demonstrated by the presence of two pseudo-radicals carried by the carbon atom C1 of value VT(C1)=1. 09e, the nitrogen number 2 (N2) also carries a monosynaptic basin of value V(N2)=3.74e, consequently the TAC is very reactive. The passage from tautomer **T-1** to tautomer **T-2** requires a very high energy of about 87 Kcal/mol, this passage reverses the bisynaptic basins between the TAC centers and becomes two

bisynaptic basins between carbon C1 and nitrogen N1 of value 4. 47e, so the C1-N1 bond becomes semi-triple bond instead of semi-double bond, the monosynaptic basin value carried by carbon C1 changes to 1.71e, thus the total amount of nitrogen N2 transported in the monosynaptic basin rises to 3.21e.

3.3. Energetical aspects

The two reactants are asymmetric, the TAC (between methyl propynoate and difluoromethyldiazomethane) can also have two tautomeric forms, so there are four cycloaddition reaction pathways 3+2, and during these pathways there occurs tautomerization either at the beginning of the reaction (the transition state **TS-T**) or during the reaction (the transition states **TS-CA32-2** and **TS-CA21**). There could also be a path of an elimination of a nitrogen molecule during a cycloaddition reaction type 2+1. Consequently, we have located eight transition states named **TS-T**, **TS-CA32-1**, **TS-CA32-F1**, **TS-CA32-2**, **TS-CA32-F2**, **TS-CA32-3** and TS-**CA32-4** and **TS-CA21**. We have also characterized the cyclic products corresponding to each transition state. The reactions activations relative energies are prearranged in **Scheme 2** and **Fig. 3** depict the profile of free energy, while the detailed calculations are given in the supplementary. **Fig. 4** shows the various geometries of the transition states localized in the cycloaddition reaction between methyl propynoate (**Alk**) and difluoromethyldiazomethane.

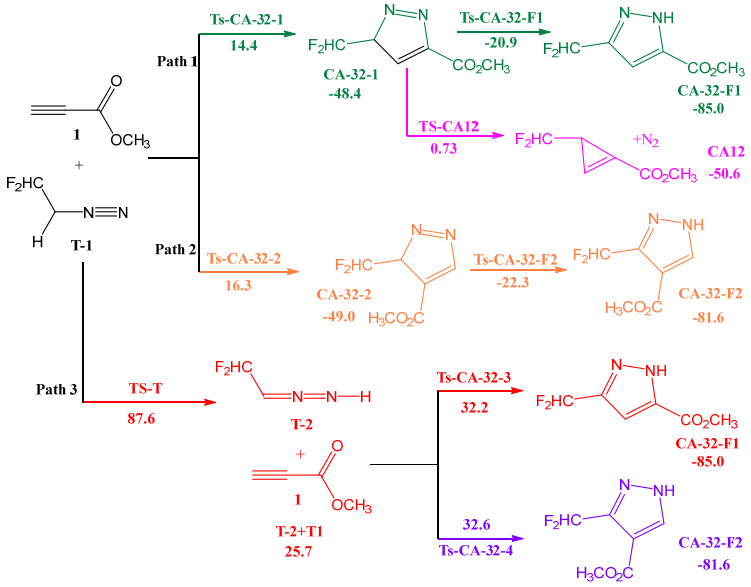

Scheme 2. Possible reaction routes in the reaction between difluoromethyldiazomethane and methyl propynoate.

The transition states **Ts-CA-32-1**, **Ts-CA-32-2**, and **Ts-T** have respective values of 14.4 kcal/mol, 16.3 kcal/mol, and 87.6 kcal/mol, indicating that **CA-32-F1** product is kinetically more favorable. The exothermic characters of these products are: **CA-32-F1** (-85.0 kcal/mol), **CA-32-F2** (-81.6 kcal/mol) and **CA21** (-50.6 kcal/mol), It demonstrates that the item **CA-32-F1** is thermodynamically favorable, thus the product **CA-32-F1** is obtained under kinetic and thermodynamic control. It should be noted that the part realized via **Ts-T** must be considered as forbidden from the kinetic point of view[71,72].

Entropy is detrimental to the bimolecular process, causes the free Gibbs relative energies to grow dramatically when the term TS is taken into account in comparison to the relative enthalpies of 12–15 kcal/mol, **Fig. 3** illustrates that the free activation energy of the [3+2] cycloaddition reaction paths between difluoromethyldiazomethane (**T-1**) and methyl propiolate (**Alk**) are: **Ts-CA32-1** (27.6 kcal/mol), **Ts-CA32-2** (30.0 kcal/mol) and **Ts-T** (84.2 kcal/mol), which shows pathway 1 is more favorable, so **CA32-1** is the preferred product, consequently the [3+2] cycloaddition reaction between difluoromethyldiazomethane **T-1** and methyl propynoate (**Alk**) is regiospecific. On the other hand the energetic difference between **Ts-CA32-1** and **Ts-T** is very big (56. 6 kcal/mol), indicates that the tautomerization reaction is impossible to realize at the beginning of this cycloaddition reaction. Therefore, the tautomeric form **T-1** of difluoromethyldiazomethane which will react with methyl propynoate (**Alk**) and consequently the tautomeric form **T-2** of difluoromethyldiazomethane is not formed in the [3+2] cycloaddition reaction between difluoromethyldiazomethane and methyl propynoate.

We obtained, from paths 1 and 2, two intermediates named **CA32-1** and **CA32-2**, which respectively have a free energy of reaction -30.1 kcal/mol and -30.5 kcal/mol, which shows that the intermediate **CA32-1** is less stable than the intermediate **CA32-2**, the intermediate **CA32-1** can be transformed by tautomerization to the product **CA32-F1** or is going to lose one molecule of nitrogen to form the product **CA21.** The energetic diference between the free energies of activation (**Ts-CA32-F1** and **Ts-CA21**) is 18.7 kcal/mol. It demonstrates that the product **CA32-F1** is much preferable than the product **CA21**, thus the tautomerization is more favorable than the removal of a nitrogen molecule in this stage. It should be noted that transformation of **CA32-1** and **CA32-2** can be formally treated as hydrogen sigmatropic shift[24,45]. The exothermic character

of the products **CA32-F1**, **CA32-F2** and **CA21** respectively in order: -66.0 kcal/mol, -61.6 kcal/mol and -47.2 kcal/mol, shows that the product **CA32-F1** is thermodynamically more favorable, this finding correlates well with the experiment.

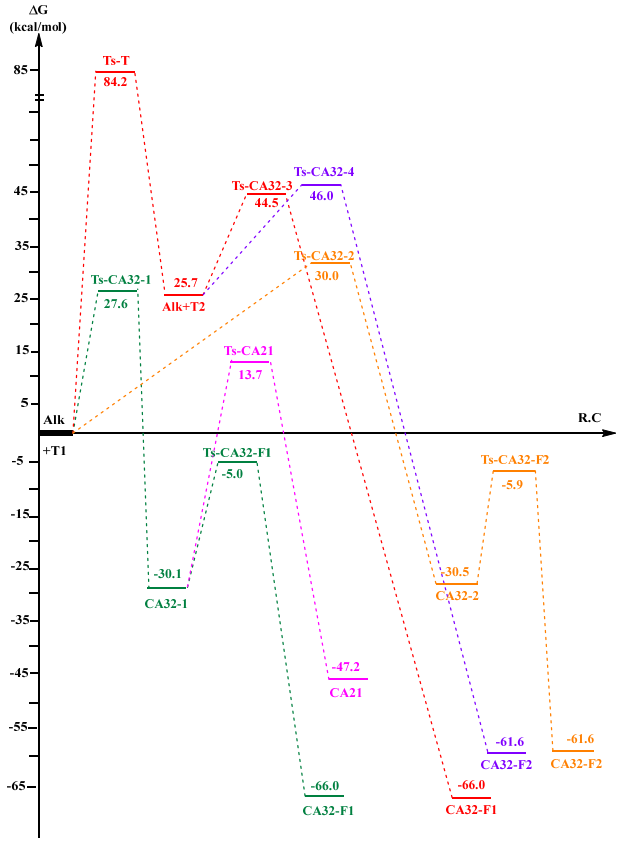

Fig. 3. Gibbs free energy profiles for the reaction of difluoromethyldiazomethane and methyl propynoate.

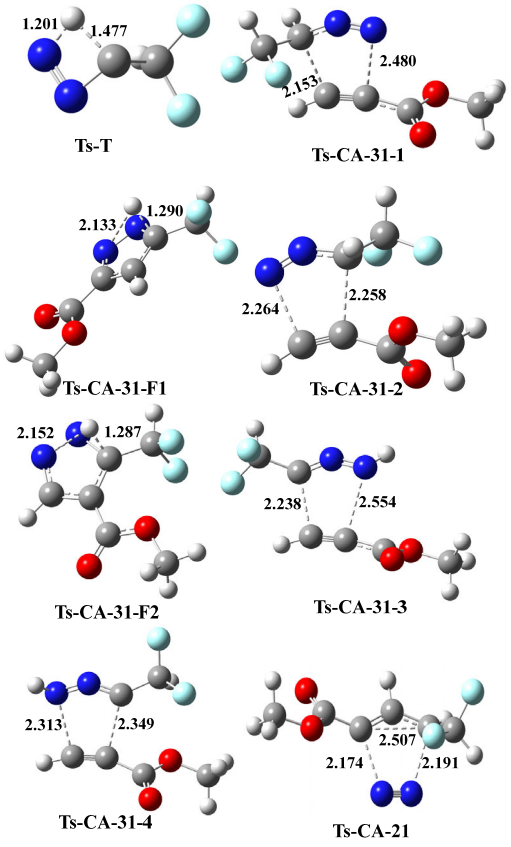

Fig. 4. Views of key structures of the reaction between methyl propynoate and difluoromethyldiazomethane in the light of DFT calculations.

3.4. Solvent effect

To estimate how this 32CA process is impacted by the solvent, we calculated the energies, enthalpies, entropy and free enthalpies of activation of path 1 that leads to the formation of the product **CA32-F1** in different solvents. We have assembled the energies and thermodynamic parameters of the reactants in **Tables S3** and **S4**, and we have tabulated these parameters of the **TS-CA31-1** transition state in **Table S5** while the different activation free energies are provided in **Table 2** and in the **Fig. 6** we presented activation free energies as a function of the dipole moment.

It can be seen in **Table 2** that the polar protic solvents have the lowest free energy of the activation followed by the polar aprotic solvents. Utilizing water as a solvent in the cycloaddition reaction between difluoromethyldiazomethane (**T-1**) and methyl propiolate (**1**) activation energy ranks about 27.84 kcal/mol, followed by methanol 27.87 kcal/mol and ethanol's activation free energy around 27.89 kcal/mol. This indicates that the use of water and ethanol as environmentally friendly solvents are as well an efficient way for considered cycloaddition reaction.

In the series of polar aprotic solvents the free energy of activations of THF, DMSO, DCM, diethyl ether, DCE, chloroform, nitromethane, acetonitrile, acetone and chlorobenzene are respectively 28.11, 27.85, 28.06, 28.29, 28.03, 28.25, 27.86, 27.87, 27.92 and 28.31 kcal/mol, showing that the solvent DMSO is the most efficient for the 32CA reaction between difluoromethyldiazomethane (**T-1**) and methyl propiolate (**Alk**), followed by Nitromethane, Acetonitrile and Acetone. In this series of solvents chlorobenzene is the least efficient.

In the series of polar solvents, the solvents' activation free energy is higher than 28 kcal/mol except cyclohexane, which has a free activation energy 27.94 kcal/mol. To conclude this part, the most efficient solvent is water. Unfortunately, there are several reagents insoluble in water, so the clear choice here should be to use DMSO or ethanolhowever, considering environment, it is recommended to use ethanol.

Table 2. Dipole moment and activation free energy for various solvents (dipole moment computed using DFT/B3LYP/6-311(d,p)).

Solvents		ΔG	(μ)
Protic polar solvents	Methanol **1**	27,87	1.71
	Ethanol **2**	27,89	1.65
	Water **3**	27,84	2.09
	Aniline **4**	28,12	1.71
Aprotic polar solvents	THF **5**	28,11	1.84
	DMSO **6**	27,85	4.14
	DCM 7	28,06	1.85
	Diethylether **8**	28,29	1.10
	DCE **9**	28,03	2.34
	Chloroform **10**	28,25	1.24
	Nitromethane **11**	27,86	3.15
	Acetonitrile **12**	27,87	3.88
	Acetone **13**	27,92	2.76
	Chlorobenzene **14**	28,31	1.97
Non-polar solvents	Toluene **15**	28,20	0.35
	Benzene **16**	28,17	0.00
	CCl4 **17**	28,05	0.00
	Cyclohexane **18**	27,94	0.00
	Heptane **19**	28,33	0.05

3.5. ELF topological exploration

To provide the description of the formation of the new single bonds along the most favorable reaction path of the 32CA reaction involving difluoromethyldiazomethane (**T-1**) and methyl propiolate (**1**), an ELF topological research of specific sites on the IRC graph was carried out.

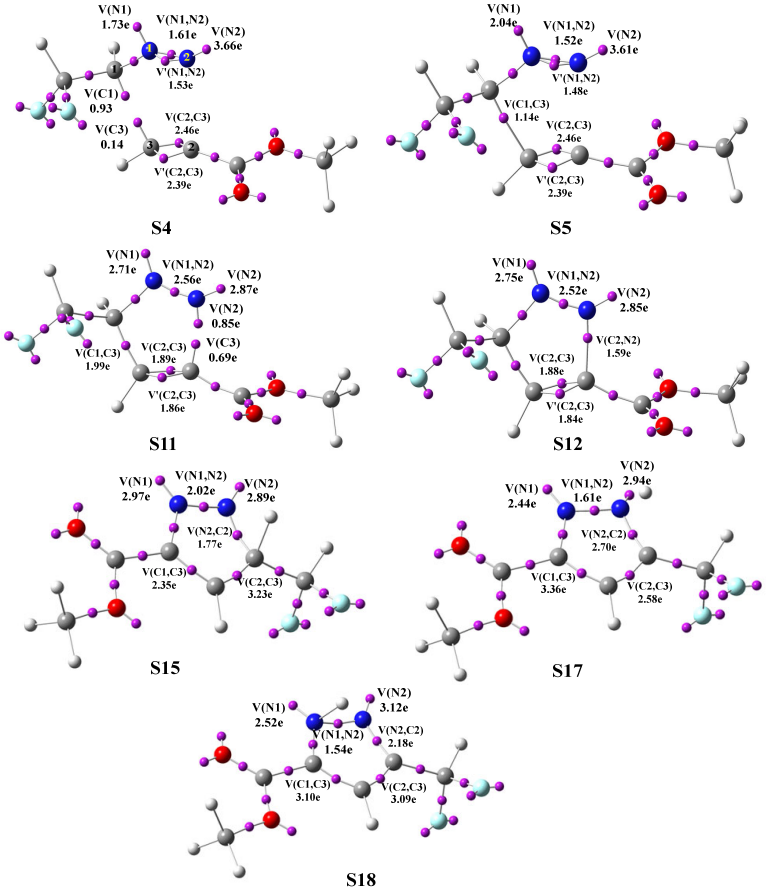

Fig. 5. The locations of the corresponding ELF basin attractors.

Fig. 5 shows the locations of the associated ELF basin attractors, whereas **Table S2** provides information on the populations of the most important ELF valence basins that contributed to the formation of the C-C and C-N single bonds in the selected structures. The S1 structure contains two monosynaptic basins carried by the C1 carbon of the diazomethane of values V(C1')=0.80e and V'(C1')=0.70e, these values are going to diminished in the S2 structure becoming V(C1')=0.60e and V(C1')=0.37e, in the S3 structure we observe the disappearance of one of the two basins carried by the C1' carbon, there remains only one monosynaptic basin of value V(C1')=0.83e, the presence of a monosynaptic basin in the structure S4 carried by the carbon C3 with the value V(C3)=0.14e.In the structure S4 we noticed the formation of the first bond between the carbon C3 of the alkyne and the carbon C1' of diazomethane, at a distance d(C1',C3) equal to 2.034 (Å), this formation is obtained starting from the union by the two monosynaptic basins carried by the two centers of the formed bond.

In structure S6, we have the formation of 77% of the C1'-C3 bond, additionally, the C2 carbon appears to be carrying a monosynaptic basin of value V(C2)=0.44e, this value increases until 0.69e in structures S10 and S11. In structure S10 we have the appearance of a second monosynaptic basin carried by the nitrogen N2 of values V(N2)=2.94e and V(N2)=0.73e, these values become V(N2)=2.87e and V'(N2)=0.85e in structure S11. In structure S12 the monosynaptic basin V'(N2) will unite with the monosynaptic basin carried by the carbon C2 to form the second bond N2-C2 at an equal distance d(N2-C2)= 1.678 (Å), this structure will relax until the product CA-32 is obtained. In the structure S15 we have the beginning of the tautomerisation, in this structure the basin V(C1',H)=1.67e, this basin will disappear in the following ones, which indicates the disappearance of the C1'-H bond, in the structure S18, we observe the appearance of a new bond between the nitrogen 2 and a hydrogen atom, thus the formation of the product **CA-321F**.

3.6. Molecular Docking Study

Our knowledge of interactions between viruses and hosts, the acute severe respiratory syndrome coronavirus 2 (SARS-CoV-2), and immune response, pathogenicity, evolution and transmission are ongoing quite restricted despite significant work over the past two years. This restriction necessitates additional study. Because of their effectiveness, low cost, and lack of safety and ethical restrictions, computational studies have emerged as a crucial tool in the fight against coronavirus 2019 (COVID-19) sickness. In order to determine potential interactions between the examined products and the Corona-Virus protein, a docking study of the products was conducted in this section.

The target COVID-19 protease protein's crystal structure in three dimensions before docking was retrieved from the Protein Data Bank at www.rcsb.org. The simulation of molecular docking was carried out with Autodockvina program[73] beside with the graphical interface AutoDockTools (ADT) version 1.5.6 accustomed to investigate substituted **CA-32-1**, **CA-32-F1**, **CA-32-2**, **CA-32-F2** and **CA-21** derivatives binding to the single-domain antibody B6 protein and the SARS-CoV-2 N protein's RNA-binding domain's 7R98 structure. Before docking protocol, the 7R98 protein was altered to remove the water molecules, atoms of polar hydrogen, followed by the addition of Kollman and Gasteiger atom charges using ADT. The grid maps were created to 40 Å in X, Y and Z directions and the center grid box is about (14.229 Å, -58.381 Å and -7.841 Å) by the ligand location in the protein. The docked molecule and its H-bond interactions were visually verified using Discovery Studio Visualizer and PyMol software, and the potential binding mechanism of our derivatives with their target proteins was demonstrated to explain their anti-Covid properties. According to docking examinations, The figure illustrates the results of docking all of the **CA-32-1**, **CA-32-F1**, **CA-32-2**, **CA-32-F2** and **CA-21** derivatives with the target 7R98 protein, whereas **Fig. 6** reveals the results of docking the **CA-32-F1**, all of the ligands interacted with the Covid-19 Protease's Ser78(A), Asn75(A), Gln83(A), and Gln40(A), which are important active site residues, the ester fragment and N atoms of the pyrazole compounds largely generated typical hydrogen bonds with the docked molecules. The bound residues, binding distances, and affinities of the investigated products are displayed in **Table 3**. Affinity of **CA-32-1, CA-32-F1, CA-32-2, CA-32-F2** and **CA-21** derivatives with the protein protease Covid-19 (PDB ID: 7R98) showed dock values between -5.9 and -4.9 kcal/mol. The following is a list of the affinity in order of therapeutic potential against 7R98: **CA-32-F1**>**CA-32-1**>**CA-32-F2**>**CA-32-2**>**CA-21**.

Table 3. The cyclic derivatives' derived docking parameters.

Product	Residual bonds	Bonding distances	Affinity (kcal/mol)
CA-32-1	- Ser78(A) - Asn75(A)	* 3.33 * 3.26 and 2.94	-5.4
CA-32-F1	- Ser78(A) - Asn75(A)	* 3.23 * 2.81	-5.9
CA-32-2	- Asn75(A) - Gln83(A) – Gln40(A)	* 3.00 * 3.03 * 3.06	-5.2
CA-32-F2	- Ser78(A) - Asn75(A)	* 3.23 * 3.14 and 2.80	-5.7
CA-21	- Asn75(A) - Gln83(A) – Gln40(A)	* 2.95 * 3.04 * 3.08	-4.7

The 7R98 protein and compound **CA-32-F1** produced a strong van der Waals connection with Ser78(A) (3.23) and a conventional hydrogen bond with Asn75(A) (2.81). The results obtained show that the **CA-32-F1** and **CA-32-F2** derivatives have a significant anti-Covid-19 activity. Design and development of new drug candidates against Covid-19 may be influenced by the docking data.

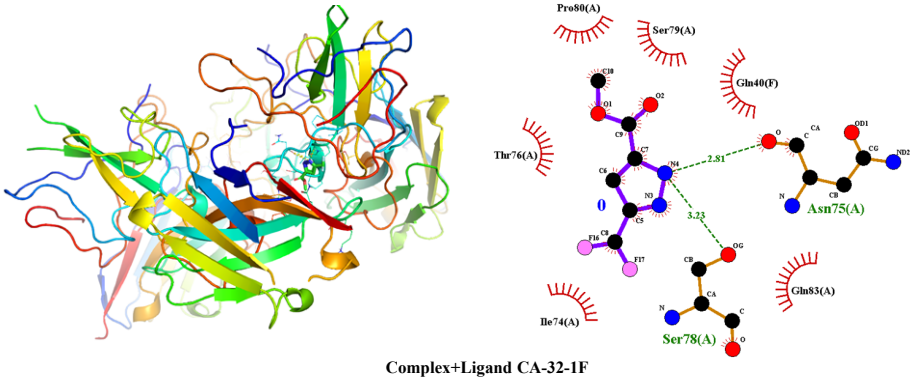

Fig. 6. Interactions between **CA-32-F1** and the major protease of COVID-19's amino acid residues.

4. Conclusions

The DFT study shed new light on the regiochemistry and molecular mechanism of the reaction between methyl propynoate and difluoromethyldiazomethane. It was found that reaction components (difluoromethyldiazomethane (**T-1**) and methyl propynoate (**1**) behave as an electrophile and a nucleophile, respectively, whereas the Mulliken atomic spin densities of the reactants methyl propynoate (**1**) and difluoromethyldiazomethane (**T-1**) demonstrate the regiospecificity of this cycloaddition reaction. All considered cycloadditions are realized via a one-step mechanism without participation of any zwitterionic or biradical intermediates independently of the polarity of the solvent. DMSO and ethanol are both extremely efficient solvents for this reaction, according to research on the subject. In complete agreement with the experimental data, the energetical analysis clearly demonstrates that the **CA-32-1** product is very favorable, showing that this cycloaddition reaction is regiospecific. Lastly, the ELF investigation suggests that the mechanism of this cycloaddition reaction is one-step but non-concerted.

Acknowledgements

The authors extend their appreciation to the Researchers Supporting Project number (RSP2023R367), King Saud University, Riyadh, Saudi Arabia.

References

1 Khan M.F., Alam M.M., Verma G., Akhtar W., Akhter M., and Shaquiquzzaman M. (**2016**) The therapeutic voyage of pyrazole and its analogs: A review. *Eur. J. Med. Chem*., 120, 170–201.
2 Heller S.T., and Natarajan S.R. (**2006**) 1,3-Diketones from acid chlorides and ketones: A rapid and general one-pot synthesis of pyra-zoles. *Org. Lett*., 8, 2675–2678.
3 Kula K., Łapczuk, A., Sadowski M., Kras J., Zawadzińska K., Demchuk O. M., Gaurav G.K., Wróblewska A. and Jasiński, R. (**2022**) On the Question of the Formation of Nitro-Functionalized 2, 4-Pyrazole Analogs on the Basis of Nitrylimine Molecular Systems and 3, 3, 3-Trichloro-1-Nitroprop-1-Ene. *Molecules*, 27(23), 8409.
4 Keter F. K., and Darkwa J. (**2012**) Perspective: The potential of pyrazole-based compounds in medicine. *Biometals*, 25, 9–21.
5 Karrouchi K., Radi S., Ramli Y., Taoufik J., Mabkhot Y.N., Al-Aizari F.A., and Ansar M. (**2018**) Synthesis and pharmacological ac-tivities of pyrazole derivatives: A Review. *Molecules,* 23, 134.
6 Faria J.V., Vegi P.F., Miguita A.G.C., Santos M.S.D., Boechat N., and Bernardino A.M.R. (**2017**) Recently reported biological activities of pyrazole compounds. *Bioorg. Med. Chem*., 25, 5891–5903.
7 Bouabdallah I., Touzani R., Zidane I., and Ramdani A. (**2007**) Effect of two isomeric tetrapyrazolyl ligands on the catalytic oxidation of 3,5-di-tert-butylcatechol. *JICS*, 4, 299–303.
8 Bennani F.E., Doudach L., Cherrah Y., Ramli Y., Karrouchi K., and Faouzi, M.E.A. (**2020**) Overview of recent developments of pyra-zole derivatives as an anticancer agent in different cell line. *Bioorg. Chem*., 97, 103470.
9 Pham E.C., Le Thi T.V., Phan L.T., Nguyen H.G.T., Le K.N., and Truong, T.N. (**2022**) Design, synthesis, antimicrobial evaluations and in silico studies of novel pyrazol-5 (4H)-one and 1H-pyrazol-5-ol derivatives. *Arab. J. Chem*., 15, 103682.
10 Ningaiah S., Bhadraiah U. K., Sobha A., and Shridevi D. (**2022**) Synthesis of novel pyrazolyl-1, 3, 4-thiadiazole analogues. *Polycycl. Aromat. Compd*., 42, 4, 1249-1259.

11 Katiyar S., Kumar A., and Sashidhara K. V. (**2022**) Silver-catalyzed decarboxylative cyclization for the synthesis of substituted pyra-zoles from 1, 2-diaza-1, 3-dienes and α-keto acids. *Chem. Comm*., 58, 52, 7297-7300.
12 Jing H., Yali L., Yijiao F., Xuezhen L. Ping L. and Bin D. (**2022**) Cs2CO3-Promoted [3 + 2] Cyclization of Chalcone and N-Tosylhydrazone, *Polycyc. Aromat. Compd*., 1.
13 Ahmed W., Yan X., Hu D., Adnan M., Tang R.Y., and Cui Z.N. (**2019**) Synthesis and fungicidal activity of novel pyrazole deriva-tives containing 5-Phenyl-2-Furan. *Bioorg. Med. Chem*., 27, 115048.
14 Titi A., Touzani R., Moliterni A., Ben Hadda T., Messal, M., Benabbes R., Berredjem M., Bouzina A., Al-Zaqri N., and Taleb, M. (**2022**) Synthesis, Structural, Biocomputational Modeling and Antifungal Activity of Novel Armed pyrazoles. *J. Mol. Struct.*, 1264, 133156.
15 Rahimizadeh M., Pordel M., Bakavoli M., Rezaeian S., and Sadeghian A. (**2010**) Synthesis and antibacterial activity of some new derivatives of pyrazole. *World J. Microbiol. Biotechnol.*, 26, 317–321.
16 Sun J., and Zhou Y. (**2015**) Synthesis and Antifungal Activity of the Derivatives of Novel Pyrazole Carboxamide and Isoxazolol Pyra-zole Carboxylate. *Molecules*, 20, 4383–4394.
17 Balbi A., Anzaldi M., Macciò C., Aiello C., Mazzei M., Gangemi R., Castagnola P., Miele M., Rosano C., and Viale M. (**2011**) Syn-thesis and biological evaluation of novel pyrazole derivatives with anticancer activity. *Eur. J. Med. Chem*., 46, 5293–5309.
18 Abdel-Aziz M., Abuo-Rahman G.E.A., and Hassan A.A. (**2009**) Synthesis of novel pyrazole derivatives and evaluation of their anti-depressant and anticonvulsant activities. *Eur. J. Med. Chem*., 44, 3480.
19 El-Moghazy S., Barsoum F., Abdel-Rahman H., and Marzouk A. (**2012**) Synthesis and anti-inflammatory activity of some pyrazole derivatives. *Med. Chem. Res.*, 21, 1722–1733.
20 Pandit U., and Dodiya A. (**2013**) Synthesis and antitubercular activity of novel pyrazole–quinazolinone hybrid analogs. *Med. Chem. Res.*, 22, 3364–3371.
21 De Oliveira D.H., Sousa F.S.S., Birmann P.T., Pesarico A.P., Alves D., Jacob R.G., and Savegnago L. (**2020**) Evaluation of antioxi-dant activity and toxicity of sulfur- or selenium-containing 4-(arylchalcogenyl)-1H-pyrazoles. *Can. J. Physiol. Pharma-col.,* 98, 441–448.
22 Ouyang G., Chen Z., Cai X.-J., Song B.-A., Bhadury P.S., Yang S., Jin L.-H., Xue W., Hu D.-Y., and Zeng S. (**2008**) Synthesis and antiviral activity of novel pyrazole derivatives containing oxime esters group. *Bioorg. Med. Chem.*, 16, 9699–9707.
23 Kula K., Dobosz J., Jasiński R., Kącka-Zych A., Łapczuk-Krygier A., Mirosław B., and Demchuk O.M. (**2020**) [3+2] Cycloaddition of diaryldiazomethanes with (E)-3,3,3-trichloro-1-nitroprop-1-ene: An experimental, theoretical and structural study. *J. Mol. Struct*., 1203, 127473.
24 Jasiński, R. (**2022**). Stepwise, zwitterionic course of hetero-Diels–Alder reaction between 1, 2, 4-triazine molecular systems and 2-cyclopropylidene-1, 3-dimethylimidazoline. *Chemistry of Heterocyclic Compounds*, 58(4-5), 260-262.
25 Fryźlewicz A., Kącka-Zych A., Demchuk O.M., Mirosław B., Woliński P., and Jasiński R. (**2021**) Green synthesis of nitrocyclopro-pane-type precursors of inhibitors for the maturation of fruits and vegetables via domino reactions of diazoalkanes with 2-nitroprop-1-ene. *J. Clean. Prod.*, 292, 126079.
26 Allaka B. S., Basavoju S., and Gamidi R. K. (**2022**) Transition Metal-and Oxidant-Free Regioselective Synthesis of 3, 4, 5-Trisubstituted Pyrazoles by Means of [3+2] Cycloaddition Reactions. *ChemistrySelect*, 7, 11, e202200605.
27 Kula K., Kącka-Zych A., Łapczuk-Krygier A., Wzorek Z., Nowak A., and Jasiński R. (**2021**) Experimental and theoretical mechanis-tic study on the thermal decomposition of 3,3-diphenyl-4-(trichloromethyl)-5-nitropyrazoline. *Molecules*, 26, 1364.
28 Zhao P., Li Z., He J., Liu X., and Feng X. (**2021**) Asymmetric catalytic 1, 3-dipolar cycloaddition of α-diazoesters for synthesis of 1-pyrazoline-based spirochromanones and beyond. *Sci. China Chem*., 64, 8, 1355-1360.
29 Kącka-Zych, A., and Jasiński, R. (**2022**). Mechanistic aspects of the synthesis of seven-membered internal nitronates via stepwise [4+3] cycloaddition involving conjugated nitroalkenes: Molecular Electron Density Theory computational study. *Journal of Computational Chemistry*, 43(18), 1221-1228.
30 Katiyar S., Kumar A., and Sashidhara K. V. (**2022**) Silver-catalyzed decarboxylative cyclization for the synthesis of substituted pyra-zoles from 1, 2-diaza-1, 3-dienes and α-keto acids. *Chem. Commun*., 58, 7297-7300.
31 Bekhit A.A., Hymete A., Bekhit A.E.A., Damtew A., and Aboul-Enein H.Y. (**2012**) Pyrazoles as Promising Scaffold for the Synthesis of Anti-Inflammatory and/or Antimicrobial Agent: A Review. *Mini Rev. Med. Chem.*, 10, 1014–1033.
32 Domingo, L. R. (**2016**) Molecular electron density theory: a modern view of reactivity in organic chemistry. *Molecules*, 21(10), 1319.
33 Ríos-Gutiérrez M., and Domingo, L. R. (**2019**) Unravelling the mysteries of the [3+ 2] cycloaddition reactions. *Eur. J. Org. Chem.*, 2019(2-3), 267-282.
34 Zeroual A., Ríos-Gutiérrez M., Salah M., El Alaoui El Abdallaoui H. and Domingo, L.R. (**2019**) An investigation of the molecular mechanism, chemoselectivity and regioselectivity of cycloaddition reaction between acetonitrile N-Oxide and 2,5-dimethyl-2H-[1,2,3]diazaphosphole: A MEDT study. *J. Chem. Sci.*, 131, 75.
35 Kącka-Zych A., and Jasiński R. (**2021**) Understanding the molecular mechanism of the stereoselective conversion of N-trialkylsilyloxy nitronates into bicyclic isoxazoline derivatives. *New J. Chem.*, 45(21), 9491-9500.
36 El Ghozlani M., Barhoumi A., Elkacmi R., Ouled Aitouna A., Zeroual A., and El Idrissi M. (**2020**) Mechanistic study of hetero-Diels–Alder [4+2] cycloaddition reactions between 2-nitro-1H-pyrrole and isoprene. *Chemistry Africa*, 3, 901-909.

37 Kula K., Kącka-Zych A., Łapczuk-Krygier A., and Jasiński R. (**2021**) Analysis of the possibility and molecular mechanism of carbon dioxide consumption in the Diels-Alder processes. *Pure Appl. Chem*., 93, 427–446.
38 Zeroual A., Ríos-Gutiérrez M., Amiri O., El Idrissi M., and Domingo, L. R. (**2019**) A molecular electron density theory study of the mechanism, chemo-and stereoselectivity of the epoxidation reaction of R-carvone with peracetic acid. *RSC Adv.*, 9, 28500-28509.
39 Zahnoune R., Asserne F., Ourhriss N., Aitouna A. O., Barhoumi A., Hakmaoui Y., Belghiti M.E., Abouricha S., El ajlaoui R., and Zeroual A. (**2022**) Theoretical survey of Diels-Alder between acrylic acid and isoprene catalyzed by the titanium tetra-chloride and titanium tertafluoride. *J. Mol. Struct.*, 1269, 133630.
40 Zeroual A. (**2021**) Theoretical investigation of the mechanism, chemo-and stereospecifity in the epoxidation reaction of limonene with meta-chloroperoxybenzoic acid (m-CPBA). *Mor. J. Chem.*, 9, 75-84.
41 Aitouna A. O., Belghiti M. E., Eşme A., Aitouna A. O., Salah M., Chekroun A., El Alaoui El Abdallaoui H., Benharref A., Mazoir N., Zeroual A., and Nejjari C. (**2021**) Divulging the regioselectivity of epoxides in the ring-opening reaction, and potential himachalene derivatives predicted to target the antibacterial activities and SARS-CoV-2 spike protein with docking study. *J. Mol. Struct*., 1244, 130864.
42 Kącka-Zych A., and Jasiński R. (**2019**) Unexpected molecular mechanism of trimethylsilyl bromide elimination from 2-(trimethylsilyloxy)-3-bromo-3-methyl-isoxazolidines. *Theor. Chem. Acc.*, 138, 81.
43 Kącka A., and Jasiński R. (**2017**) A dramatic change of kinetic conditions and molecular mechanism of decomposition processes of ni-troalkyl carboxylates catalyzed by ethylammonium cations. *Comput. Theor. Chem*., 1104, 37-42.
44 Kącka-Zych A., and Jasiński R. (**2021**) Understanding the molecular mechanism of γ-elimination of nitrous acid in the framework of the molecular electron density theory. *J. Comput. Chem.*, 42(17), 1195-1203.
45 Jasiński R. (**2018**) β-Trifluoromethylated nitroethenes in Diels-Alder reaction with cyclopentadiene: A DFT computational study. *J. Fluor. Chem.*, 206, 1-7.
46 Mykhailiuk, P. K. (**2015**) In Situ Generation of Difluoromethyl Diazomethane for [3+2] Cycloadditions with Alkynes. Angewandte Chemie International Edition*,* 54(22)*, 6558–6561.*
47 Jasiński, R. (**2016**) A reexamination of the molecular mechanism of the Diels–Alder reaction between tetrafluoroethene and cyclopentadiene. *React. Kinet. Mech. Catal.*, 119, 49-57.
48 Jasiński R. (**2020**) A new insight on the molecular mechanism of the reaction between (Z)-C,N-diphenylnitrone and 1,2-bismethylene-3,3,4,4,5,5-hexamethylcyclopentane. *J. Mol. Graph. Model.*, 94, 107461.
49 Woliński P., Kącka-Zych A., Demchuk O.M., Łapczuk-Krygier A., Mirosław B., and Jasiński R. (**2020**) Clean and molecularly pro-grammable protocol for preparation of bis-heterobiarylic systems via a domino pseudocyclic reaction as a valuable alternative for TM-catalyzed cross-couplings. *J. Clean. Prod*., 275, 122086.
50 Kula K., and Łapczuk-Krygier A. (**2018**) A DFT computational study on the [3+2] cycloaddition between parent thionitrone and ni-troethene. *Curr. Chem. Lett*., 7, 27–34.
51 Jasiński R. (**2018**) Competition between one-step and two-step mechanism in polar [3+2] cycloadditions of (Z)-C-(3,4,5-trimethoxyphenyl)-N-methyl-nitrone with (Z)-2-EWG-1-bromo-1-nitroethenes. *Comput. Theor. Chem*., 1125, 77–85.
52 Jasiński R. (**2015**) In the searching for zwitterionic intermediates on reaction paths of 32CAreactions between 2,2,4,4-tetramethyl-3-thiocyclobutanone S-methylide and polymerizable olefins. *RSC Adv.*, 5, 101045–101048.
53 Jasiński R. (**2015**) A stepwise, zwitterionic mechanism for the 1,3-dipolar cycloaddition between (Z)-C-4-methoxyphenyl-N-phenylnitrone and gem-chloronitroethene catalysed by 1-butyl-3-methylimidazolium ionic liquid cations. *Tetrahedron Lett.*, 56, 532–535.
54 Jasiński R. (**2015**) Nitroacetylene as dipolarophile in [2+3] cycloaddition reactions with allenyl-type three-atom components: DFT computational study. *Monatshefte für Chemie*, 146, 591–599.
55 McLean A.D. (**1980**) Contracted Gaussian basis sets for molecular calculations. I. Second row atoms, Z = 11–18. *J. Chem. Phys.*, 72, 5639–5648.
56 Krishnan R.B.J.S., Binkley J.S., Seeger R., and Pople J.A. (**1980**) Self-consistent molecular orbital methods. XX. A basis set for correlated wave functions. *J. Chem. Phys.*, 72, 650–654.
57 Frisch M. J., Trucks G. W., Schlegel H. B., Scuseria G. E., Robb M. A., Cheeseman J. R., Montgomery J. A., Vreven T. J., Kudin K. N., Burant J. C., Millam J. M., Iyengar S. S., Tomasi J., Barone V., Mennucci B., Cossi M., Scalmani G., Rega N., Petersson G. A., Nakatsuji H., Hada M., Ehara M., Toyota K., Fukuda R., Hasegawa J., Ishida M., Nakajima Y., Honda O., Kitao O., Nakai H., Klene M., Li X., Knox J. E., Hratchian H. P., Cross J. B., Adamo C., Jaramillo J., Gomperts R., Stratmann R. E., Yazyev O., Austin A. J., Cammi R., Pomelli C., Ochterski J. W., Ayala P. Y., Morokuma K., Voth G. A., Salvador P., Dannenberg J. J., Zakrzewski V. G., Dapprich S., Daniels A. D., Strain M. C., Farkas M. C., Malick D. K., Rabuck A. D., Raghavachari K., Foresman J. B., Ortiz J. V., Cui Q., Baboul A. G., Clifford S., Cioslowski J., Stefanov B. B., Liu G., Liashenko A., Piskorz P., Komaromi I., Martin R. L., Fox D. J., Keith T., Al-Laham M. A., Peng C. Y., Nanayakkara A., Challacombe M., Gill P. M. W., Johnson B., Chen W., Wong M. W., Gonzalez C., and Pople J. A. (**2009**) Gaussian 09 rev A.1 Gaussian Inc. Wallingford CT, USA.
58 Schlegel H.B. (**1982**) Optimization of equilibrium geometries and transition structures. *J. Comput. Chem*., 3, 214–218.
59 Schlegel H.B. (**1994**) *Modern Electronic Structure Theory*. Yarkony, D.R., Ed.; World Scientific Publishing: Singapore.
60Tomasi J., and Persico M. (**1994**) Molecular interactions in solution: And overview of methods based on continuous distributions of the solvent. *Chem. Rev.*, 94, 2027–2094.
61 Cossi M., Barone V., Cammi R., and Tomasi J. (**1996**) Ab initio study of solvated molecules: A new implementation of the polarizable continuum model. *Chem. Phys. Lett.*, 255, 327–335.
62 Cances E., Mennucci B., and Tomasi J. (**1997**) A new integral equation formalism for the polarizable continuum model:

Theoretical background and applications to isotropic and anisotropic dielectrics. *J. Chem. Phys.*, 107, 3032–3041.
63 Barone V., Cossi M., and Tomasi J. (**1998**) Geometry optimization of molecular structures in solution by the polarizable continuum model. *J. Comput. Chem*, 19, 404–417.
64 Parr R.G., and Yang W. (**1989**) *Density Functional Theory of Atoms and Molecules*. Oxford University Press: New York, USA.
65 Domingo L.R., Chamorro E., and Pérez P. (**2008**) Understanding the reactivity of captodative ethylenes in polar cycloaddition reac-tions. A theoretical study. *J. Org. Chem.*, 73, 4615–4624.
66 Domingo L.R., Perez P., and Sáez J.A. (**2013**) Understanding the local reactivity in polar organic reactions through electrophilic and nucleophilic Parr functions. *RSC Adv.*, 3, 1486–1494.
67 Zeroual A., Zoubir M., Hammal R., Benharref A., and El Hajbi A. (**2015**) Understanding the regioselectivity and reactivity of Friedel–Crafts benzoylation using Parr functions. *Mor. J. Chem*, 3, 356-360.
68 Becke A.D., and Edgecombe K.E. (**1990**) A simple measure of electron localization n atomic and molecular-systems. *J. Chem. Phys.*, 92, 5397–5403.
69 Noury S., Krokidis X., Fuster F., and Silvi B. (**1999**) Computational tools for the electron localization function topological analy-sis. *Comput. Chem.*, 23, 597–604.
70 Domingo L. R., and Ríos-Gutiérrez M. A (**2023**) Useful Classification of Organic Reactions Based on the Flux of the Electron Density. *Scientiae Radices*, 2, 1-24.
71 Jasiński, R. (**2015**) A stepwise, zwitterionic mechanism for the 1, 3-dipolar cycloaddition between (Z)-C-4-methoxyphenyl-N-phenylnitrone and gem-chloronitroethene catalysed by 1-butyl-3-methylimidazolium ionic liquid cations. *Tetrahedron Lett.*, 56(3), 532-535.
72 Jasiński, R. (**2014**) Searching for zwitterionic intermediates in Hetero Diels–Alder reactions between methyl α, p-dinitrocinnamate and vinyl-alkyl ethers. *Computational and Theoretical Chemistry*, *1046*, 93-98.
73 Butt S.S., Badshah Y., Shabbir M., and Rafiq M. (**2020**) Molecular Docking Using Chimera and Autodock Vina Software for Nonbio-informaticians. *JMIR Bioinform. Biotechnol*., 1, e14232.